



OPEN

## Solubilities of CO<sub>2</sub>, O<sub>2</sub> and N<sub>2</sub> in rocket propellant 5 under low pressure

Chaoyue Li<sup>1,2</sup>, Shiyu Feng<sup>2✉</sup>, Lei Xu<sup>1</sup>, Xiaotian Peng<sup>2</sup> & Weihua Liu<sup>2</sup>

The static method of isochoric saturation was used to measure the solubilities of CO<sub>2</sub>, O<sub>2</sub> and N<sub>2</sub> in rocket propellant 5 (RP5) at temperatures ranging from 253.15 to 323.15 K in 10 K intervals and pressures ranging from 0 to 120 kPa. The measurement accuracy of the constructed experimental setup was verified by measuring the solubility of CO<sub>2</sub> in water. The relative expanded uncertainty ( $k=2$ ) in the solubility data was less than 4.0%. The solubilities of CO<sub>2</sub>, O<sub>2</sub> and N<sub>2</sub> in RP5 increased with pressure. As the temperature increased, the solubility decreased for CO<sub>2</sub> solubility and increased for O<sub>2</sub> and N<sub>2</sub>. Henry's constants for the three gases in RP5 decreased over the experimental temperature and pressure ranges in the order of N<sub>2</sub>>O<sub>2</sub>>CO<sub>2</sub>. The measured solubilities of CO<sub>2</sub>, O<sub>2</sub> and N<sub>2</sub> could be fitted with a modified Krichevsky–Kasarnovsky equation, and the maximum deviation between the measured and calculated data was less than 8.04%, 7.03% and 6.18%, respectively.

Fuel tank combustion explosions are one of the main causes of aircraft safety accidents. The gas mixture of air and fuel vapor in the tank ullage becomes highly combustible in the presence of an external ignition source for oxygen concentrations (volume fractions) above the limiting oxygen concentration (12% for passenger planes and 9% for military aircraft)<sup>1,2</sup>. The results of extensive experiments and calculations have shown that fuel tank inerting is a reasonable and potentially cost-effective approach to reduce fuel tank flammability<sup>3–5</sup>. Fuel tank inerting involves injecting inert gases, such as CO<sub>2</sub> and N<sub>2</sub>, into a fuel tank to replace the oxygen in ullage, thereby reducing the oxygen concentration below the limiting value. The dissolved gases CO<sub>2</sub>, O<sub>2</sub> and N<sub>2</sub> will escape from jet fuel under variations of the ambient pressure and temperature, which has a negative effect on the analysis of fuel tank flammability<sup>6,7</sup>. Knowledge of the solubilities of CO<sub>2</sub>, O<sub>2</sub> and N<sub>2</sub> in jet fuel under low pressure is essential for analyzing variations in the oxygen concentration in the ullage. Therefore, it is critical to obtain solubility data to improve the design of aircraft fuel tank inerting systems.

RP5 is a hydrocarbon fuel with a high density, viscosity, heat of combustion, and flash point that is widely used in carrier-based aircraft in China<sup>8</sup>. However, the dissolution characteristics of this fuel depend strongly on the material composition, temperature and pressure, and no universally accurate model is available to predict the gas solubility in RP5 from other known solubility data<sup>9,10</sup>. Barth<sup>11</sup> measured the solubility of methane in diesel fuel and it was compared to that of methane in pure hexadecane which is similar to diesel fuel with respect to the mean carbon number, and the solubility of methane in diesel fuel is smaller than that of methane in hexadecane. Baird<sup>12</sup> studied the hydrogen solubility of shale oil and found that the shale oil had a lower hydrogen solubility than most other fuels probably due to the high content of polar phenolic compounds in the oil. Hamme<sup>13</sup> studied the solubility of neon, nitrogen and argon in distilled water and seawater, and found that the solubility data could be expressed as a polynomial function of temperature and salinity. Thus, experimental tests are necessary to obtain the solubilities of CO<sub>2</sub>, O<sub>2</sub> and N<sub>2</sub> in RP5.

Many experimental setups have been developed to measure solubility, such as headspace gas chromatography<sup>14</sup>, absolute gravimetric<sup>15</sup> and isochoric saturation methods<sup>16,17</sup>. The isochoric saturation method offers the advantages of simple operation, a low experimental cost and high accuracy over other methods and is thus widely used to measure gas solubility in liquids. Liu et al.<sup>18</sup> measured the solubilities of oxygen, nitrogen and carbon dioxide in JP-10 jet fuel at temperatures ranging from 293 to 343 K and pressures ranging from 0.5 to 7.5 MPa. Jia et al.<sup>19</sup> investigated the solubilities of carbon dioxide, oxygen and nitrogen in aqueous ethylene glycol solution at temperatures ranging from 263 to 293 K and pressures ranging from 9 to 101 kPa. Shokouhi et al.<sup>20</sup> experimentally determined the solubility of hydrogen sulfide in aqueous sulfolane solution from 303.15 to 353.15 K and at pressures up to 2 MPa.

<sup>1</sup>School of Mechanical and Electrical Engineering, Jinling Institute of Technology, Nanjing 211169, China. <sup>2</sup>School of Aerospace Engineering, Nanjing University of Aeronautics and Astronautics, Nanjing 210016, China. ✉email: shiyuf@nuaa.edu.cn

| Chemical name   | Source   | Mass fraction purity (%) | CAS number |
|-----------------|--|--------------------------|------------|
| CO <sub>2</sub> | Nanjing Tianze Gas Company                                     | 99.99                    | 124-38-9   |
| O <sub>2</sub>  |  | 99.99                    | 7782-44-7  |
| N <sub>2</sub>  |  | 99.99                    | 7727-37-9  |
| RP5             | AVIC Jincheng Nanjing Engineering Institute of Aircraft System | 99                       | 8008-20-6  |

**Table 1.** Information on materials used in the experiment.

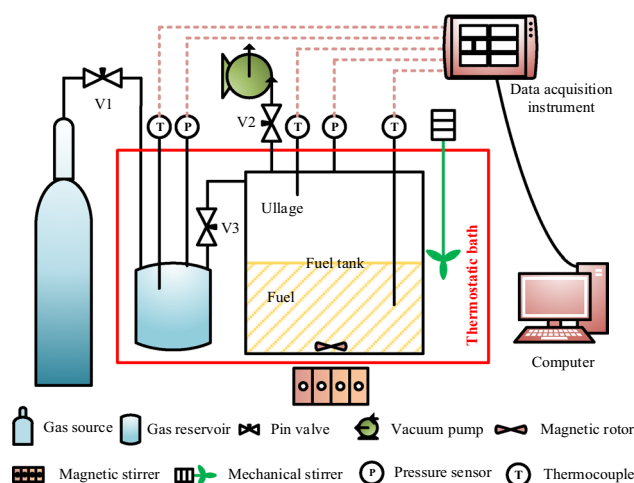


**Figure 1.** Schematic of experimental system for measuring solubility.

An isochoric saturation method was used in this study to measure the solubilities of CO<sub>2</sub>, O<sub>2</sub> and N<sub>2</sub> in RP5 at temperatures ranging from 253.15 to 323.15 K and pressures ranging from 0 to 120 kPa. The experimental solubility data could be fitted with a modified Krichevsky–Kasarnovsky equation, and Henry's constant for solvation was calculated at different temperatures.

## Experimental section

**Materials.** The CO<sub>2</sub>, O<sub>2</sub> and N<sub>2</sub> used in the experiment were purchased from Nanjing Tianze Gas Company with purities above 99.99%. The RP5 was provided by the AVIC Jincheng Nanjing Engineering Institute of Aircraft System with a mass fraction purity of 99%. The RP5 is composed of 78.5% (volume fraction) saturated hydrocarbons, 1.8% unsaturated hydrocarbons and 19.7% aromatic hydrocarbons, that are provided by suppliers. The average molecular mass of RP5 is 155. Information on the experimental materials used in this study is presented in Table 1.

**Experimental apparatus and method.** The isochoric saturation method was used to measure the solubilities of CO<sub>2</sub>, O<sub>2</sub> and N<sub>2</sub>, where the experimental system is presented in Fig. 1. The experimental apparatus consists of a gas source, a gas reservoir, a fuel tank, three pin valves, a vacuum pump, a magnetic rotor, a magnetic stirrer, a thermostatic bath (FDL BC-3006), three thermocouples (Model K), two pressure sensors (HSTL-800), a data acquisition system and a computer.

The water storage method was used to measure the volumes of the gas reservoir and fuel tank, including the line and valves. Disconnecting the gas reservoir from fuel tank and degassed water is injected into the gas reservoir from valve 1 until the gas reservoir is filled. The volume of gas reservoir could be measured by measuring the volume of water and repeated three times. The same method is applied to measure the volume of the fuel tank. The volumes of the gas reservoir and fuel tank are  $332 \pm 0.2$  mL and  $469 \pm 0.2$  mL, respectively. A thermostatic bath is used to maintain a constant temperature in the fuel tank with an error range of 0.02 K. The test range of the thermocouple is 243.15–373.15 K with the precision of 0.02 K. The test range of the pressure sensor in the gas reservoir is 0–400 kPa with a precision of 0.1 kPa over the full pressure range.

The gas tightness of the experimental system is checked before making measurements by injecting compressed air at 300 kPa into the system; the experimental requirements are met if the pressure drop is less than 1 kPa after 24 h<sup>18</sup>. First, approximately 260 g of RP5 are poured into the fuel tank, and the temperature of the thermostatic bath is set to the experimental temperature. Second, the air in the gas reservoir and fuel tank is degassed by a vacuum pump, and dissolved air escapes from the fuel because of the decrease in the pressure. Third, V1 is opened, V3 is closed, and either CO<sub>2</sub>, O<sub>2</sub> or N<sub>2</sub> is loaded into the gas reservoir at the given temperature and pressure. Finally, V3 is opened to transfer gas into the fuel tank, and the pressure decreases as the gas dissolves

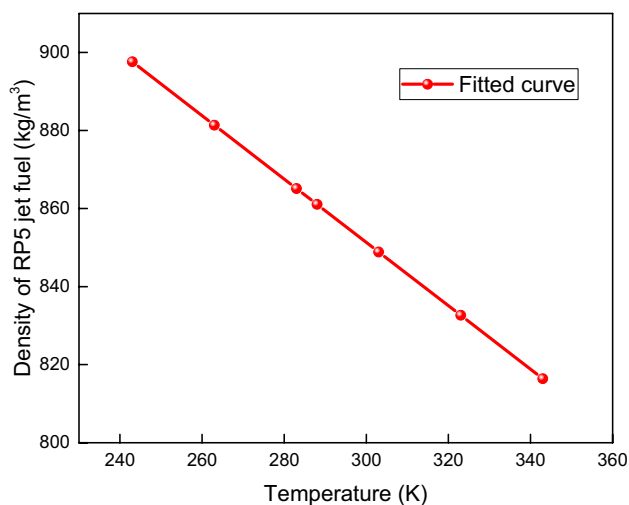


**Figure 2.** Density of RP5 versus temperature.

in the fuel and reaches solution equilibrium. A magnetic stirrer is turned on during the experiment to accelerate the dissolution of  $\text{CO}_2$ ,  $\text{O}_2$  or  $\text{N}_2$  in RP5 until the temperature and pressure no longer change.

The gas solubility in PR5 is presented as a mole fraction, that is, the ratio of the number of moles of dissolved gas to the total number of moles of gas and fuel. The gas solubility can be expressed as follows:

$$x = \frac{n_{g,d}}{n_{g,d} + n_1} \quad (1)$$

where  $x$  is the mole fraction;  $n_{g,d}$  is the number of moles of gas dissolved in fuel; and  $n_1$  is the number of moles of fuel.

The fuel mole number is calculated as follows:

$$n_1 = \frac{m_1}{M_1} \quad (2)$$

where  $m_1$  is the mass of the fuel, kg; and  $M_1$  is the molecular mass of the fuel.

The mole number of the dissolved gas can be expressed as follows:

$$n_{g,d} = \frac{(\rho_{g,i} - \rho_{g,f})V_G - \rho_{g,u}V_u}{M_g} \quad (3)$$

where  $\rho_{g,i}$  and  $\rho_{g,f}$  are the densities of the gas in the gas reservoir before and after transfer to the fuel tank, respectively,  $\text{kg/m}^3$ ;  $\rho_{g,u}$  is the density of gas in the fuel tank ullage after the transfer; and  $V_G$  and  $V_u$  are the volume of the gas reservoir and the fuel tank ullage, respectively,  $\text{m}^3$ ;  $M_g$  is the molecular mass of gas.

The gas densities  $\rho_{g,i}$  and  $\rho_{g,f}$  at a given temperature and pressure can be obtained from REFPROP 9.1<sup>21</sup>. The fuel tank ullage can be written as follows:

$$V_u = V_f - V_1 \quad (4)$$

where  $V_f$  is the fuel tank volume,  $\text{m}^3$ ; and  $V_1$  is the volume of the liquid PR5 jet fuel,  $\text{m}^3$ .

The fuel volume can be expressed as follows:

$$V_1 = \frac{m_1}{\rho_1} \quad (5)$$

where  $\rho_1$  is the density of fuel,  $\text{kg/m}^3$ .

The temperature dependence of the RP5 density affects the fuel volume calculation. Therefore, to determine the solubility accurately, the RP5 density was measured using a DA-300API electronic densitometer at temperatures ranging from 243.15 to 343.15 K and atmospheric pressure. The experimental data for the density versus temperature shown in Fig. 2 could be fitted with a linear function as follows:

$$\rho_1 = 1094.92 - 0.81T \quad (6)$$

where  $T$  is the temperature, K.

The mole fraction  $x$  of gas dissolved in the fuel can thus be expressed as follows:

$$x = \frac{(\rho_{g,i} - \rho_{g,f})V_G - \rho_{g,u}(V_f - V_1)}{M_g n_1 + V_G(\rho_{g,i} - \rho_{g,f}) - \rho_{g,u}(V_f - V_1)} \quad (7)$$

| T/K    | p/kPa  | x      | U(x)/×10 <sup>-4</sup> |
|--------|--------|--------|------------------------|
| 283.12 | 259.65 | 0.0035 | 1.35                   |
| 283.16 | 176.71 | 0.0015 | 1.24                   |
| 293.15 | 223.56 | 0.0017 | 1.19                   |
| 293.17 | 156.23 | 0.0012 | 1.05                   |
| 303.18 | 273.52 | 0.0016 | 2.15                   |
| 303.16 | 200.35 | 0.0012 | 1.98                   |
| 313.15 | 321.38 | 0.0027 | 3.56                   |
| 313.14 | 184.88 | 0.0017 | 3.21                   |
| 323.13 | 335.12 | 0.0023 | 3.05                   |
| 323.19 | 196.57 | 0.0014 | 2.98                   |

**Table 2.** Solubility (mole fraction) of CO<sub>2</sub> in water.

The expanded uncertainty in the solubility mole fraction  $U(x)$  can be expressed as follows<sup>22</sup>:

$$U(x) = ku(x) = k\sqrt{\sum u_i^2(x)} \quad (8)$$

where  $U(x)$  is the expanded uncertainty in the mole fraction;  $k$  is the coverage factor that can be considered as 2;  $u(x)$  is the combined standard uncertainty; and  $u_i(x)$  is the uncertainty in each influencing factor.

Equations (1)–(7) can be combined to express  $U(x)$  as follows:

$$U(x) = k\sqrt{\left(\frac{\delta x}{\delta V_G}\right)^2 u^2(V_G) + \left(\frac{\delta x}{\delta \rho_{g,i}}\right)^2 u^2(\rho_{g,i}) + \left(\frac{\delta x}{\delta \rho_{g,f}}\right)^2 u^2(\rho_{g,f}) + \left(\frac{\delta x}{\delta \rho_{g,u}}\right)^2 u^2(\rho_{g,u}) + \left(\frac{\delta x}{\delta V_f}\right)^2 u^2(V_f) + \left(\frac{\delta x}{\delta V_1}\right)^2 u^2(V_1) + \left(\frac{\delta x}{\delta m}\right)^2 u^2(m)} \quad (9)$$

The expanded uncertainties in the measurement variables in the experiment are as follows: temperature (0.023 K), mass of RP5 (0.00002 g), pressure (0.12 kPa), volume of gas reservoir and fuel tank (0.2 mL), density of CO<sub>2</sub> (0.1%), density of O<sub>2</sub> (0.06%), and density of N<sub>2</sub> (0.04%). The relative expanded uncertainty in the experimental solubility data is less than 4.0% when  $k$  is 2 (In general, the value of the coverage factor  $k$  is chosen on the basis of the desired level of confidence to be associated with the interval defined by  $U = kuc$ . Typically,  $k$  is in the range 2–3. When the normal distribution applies and  $uc$  has negligible uncertainty,  $U = 2uc$  ( $k = 2$ ) defines an interval having a level of confidence of approximately 95%. To be consistent with current international practice, the value of  $k$  to be used at NIST for calculating  $U$  is, by convention,  $k = 2$ <sup>22</sup>).

**Ethics approval.** The research for this article do not include human or animal subjects.

**Verification of accuracy of experimental apparatus.** To verify the accuracy of the apparatus for measuring gas solubility in RP5, the solubility of CO<sub>2</sub> in water was measured using the experimental system at temperatures ranging from 283.15 to 323.15 K and pressures ranging from 30 to 340 kPa; the results are shown in Table 2.

Figure 3 is a comparison of the experimental data against data obtained from the literature<sup>19</sup>, where the average relative deviation and maximum deviation are 3.89% and 6.81%, respectively. Therefore, the experimentally obtained solubility of CO<sub>2</sub> in water agrees well with the literature values, and the accuracy of the apparatus meets solubility measurement requirements.

## Results and discussion

**Experimental solubility.** The solubilities of CO<sub>2</sub>, O<sub>2</sub> and N<sub>2</sub> in RP5 were measured at temperatures ranging from 253.15 to 323.15 K and pressures ranging from 0 to 120 kPa. The experimental data and the expanded uncertainties in the mole fraction are listed in Tables 3, 4 and 5. The solubility data versus temperature and pressure are presented in Figs. 4, 5 and 6.

The solubilities of the three gases in RP5 clearly increase with pressure. The mole fraction of CO<sub>2</sub> in RP5 decreases with increasing temperature. By contrast, the mole fractions of O<sub>2</sub> and N<sub>2</sub> in RP5 increase with temperature. Figure 7 shows the solubilities of CO<sub>2</sub>, O<sub>2</sub> and N<sub>2</sub> in RP5 at 293.15 K, where the gas solubility decreases in the order CO<sub>2</sub> > O<sub>2</sub> > N<sub>2</sub> at the same temperature and pressure. The solubility of CO<sub>2</sub> in RP5 increase faster than those of O<sub>2</sub> and N<sub>2</sub> as pressure increase, which indicates the solubility of CO<sub>2</sub> in RP5 is more sensitive to pressure.

**Solubility data analysis.** Henry's law is the most commonly used correlation for evaluating the solubility of a gas dissolved in a liquid solvent. A more general form of Henry's law that accounts for pressure effects is based on a thermodynamic correlation known as the Krichevsky–Kasarnovsky equation<sup>9,23,24</sup> and can be expressed as follows:

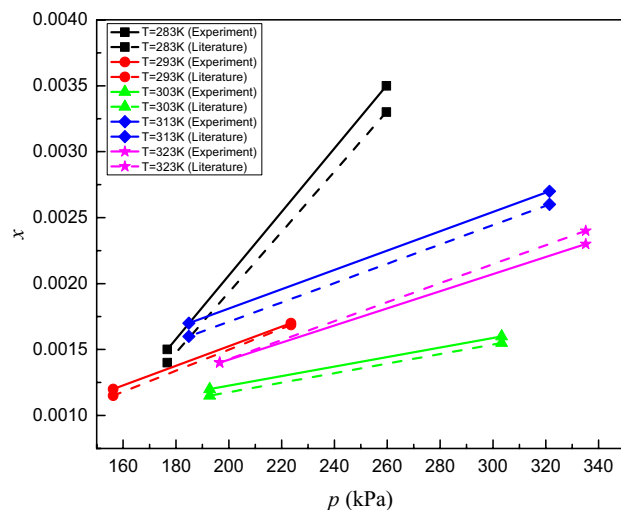


**Figure 3.** Comparisons of the experimental solubility (mole fraction) of CO<sub>2</sub> in water with data from the literature.

| T/K    | p/kPa   | $x/\times 10^{-3}$ | $U(x)/\times 10^{-3}$ | T/K    | p/kPa   | $x/\times 10^{-3}$ | $U(x)/\times 10^{-3}$ |
|--------|---------|--------------------|-----------------------|--------|---------|--------------------|-----------------------|
| 253.15 | 45.287  | 18.26              | 0.035                 | 293.25 | 28.550  | 7.35               | 0.062                 |
| 253.25 | 84.922  | 35.61              | 0.042                 | 293.15 | 58.493  | 15.85              | 0.068                 |
| 253.15 | 97.628  | 42.71              | 0.047                 | 293.15 | 87.195  | 24.17              | 0.075                 |
| 263.15 | 44.659  | 16.41              | 0.058                 | 303.15 | 32.208  | 7.81               | 0.055                 |
| 263.15 | 77.842  | 29.22              | 0.062                 | 303.15 | 74.180  | 16.58              | 0.062                 |
| 263.25 | 103.574 | 38.05              | 0.069                 | 303.15 | 94.527  | 22.07              | 0.071                 |
| 273.15 | 30.408  | 9.31               | 0.049                 | 313.15 | 28.991  | 6.49               | 0.061                 |
| 273.15 | 72.079  | 24.16              | 0.063                 | 313.15 | 74.385  | 16.14              | 0.063                 |
| 273.25 | 104.280 | 34.18              | 0.071                 | 313.15 | 112.058 | 24.97              | 0.073                 |
| 283.15 | 46.807  | 12.45              | 0.056                 | 323.35 | 48.205  | 9.73               | 0.046                 |
| 283.15 | 60.184  | 17.56              | 0.074                 | 323.15 | 67.185  | 13.44              | 0.051                 |
| 283.25 | 86.276  | 24.82              | 0.079                 | 323.15 | 90.207  | 16.83              | 0.058                 |

**Table 3.** Solubility (mole fraction) and associated uncertainty of CO<sub>2</sub> in RP5.

| T/K    | p/kPa  | $x/\times 10^{-3}$ | $U(x)/\times 10^{-3}$ | T/K    | p/kPa  | $x/\times 10^{-3}$ | $U(x)/\times 10^{-3}$ |
|--------|--------|--------------------|-----------------------|--------|--------|--------------------|-----------------------|
| 253.45 | 45.667 | 0.54               | 0.0048                | 293.35 | 39.499 | 0.52               | 0.0041                |
| 253.15 | 84.285 | 1.02               | 0.0051                | 293.15 | 64.228 | 0.90               | 0.0052                |
| 253.15 | 97.374 | 1.21               | 0.0069                | 293.15 | 94.877 | 1.29               | 0.0062                |
| 263.05 | 27.550 | 0.36               | 0.0044                | 303.15 | 28.540 | 0.42               | 0.0066                |
| 263.15 | 58.944 | 0.73               | 0.0053                | 303.15 | 67.991 | 0.94               | 0.0073                |
| 263.15 | 96.334 | 1.27               | 0.0065                | 303.25 | 87.997 | 1.20               | 0.0078                |
| 273.25 | 40.281 | 0.53               | 0.0032                | 313.15 | 42.556 | 0.59               | 0.0047                |
| 273.35 | 66.810 | 0.87               | 0.0054                | 313.35 | 67.220 | 0.93               | 0.0058                |
| 273.15 | 97.224 | 1.26               | 0.0065                | 313.15 | 87.366 | 1.24               | 0.0078                |
| 283.25 | 36.331 | 0.51               | 0.0058                | 323.15 | 45.230 | 0.62               | 0.0033                |
| 283.35 | 74.112 | 1.02               | 0.0071                | 323.25 | 67.589 | 0.94               | 0.0048                |
| 283.15 | 95.352 | 1.27               | 0.0071                | 323.15 | 91.254 | 1.32               | 0.0055                |

**Table 4.** Solubility (mole fraction) and associated uncertainty of O<sub>2</sub> in RP5.

| T/K    | p/kPa  | $x/\times 10^{-3}$ | $U(x)/\times 10^{-3}$ | T/K    | p/kPa  | $x/\times 10^{-3}$ | $U(x)/\times 10^{-3}$ |
|--------|--------|--------------------|-----------------------|--------|--------|--------------------|-----------------------|
| 253.35 | 19.250 | 0.099              | 0.0031                | 293.25 | 39.550 | 0.98               | 0.0025                |
| 253.15 | 48.633 | 0.259              | 0.0044                | 293.25 | 76.267 | 1.93               | 0.0050                |
| 253.25 | 85.799 | 0.480              | 0.0053                | 293.15 | 86.411 | 2.06               | 0.0053                |
| 263.15 | 28.336 | 0.153              | 0.0070                | 303.15 | 26.331 | 0.72               | 0.0018                |
| 263.15 | 61.083 | 0.335              | 0.0079                | 303.25 | 58.740 | 1.60               | 0.0041                |
| 263.35 | 89.926 | 0.519              | 0.0091                | 303.15 | 82.669 | 2.19               | 0.0057                |
| 273.15 | 29.994 | 0.182              | 0.0052                | 313.35 | 34.441 | 0.96               | 0.0025                |
| 273.25 | 67.240 | 0.415              | 0.0068                | 313.15 | 60.285 | 1.69               | 0.0044                |
| 273.15 | 84.685 | 0.512              | 0.0079                | 313.25 | 76.338 | 2.10               | 0.0054                |
| 283.15 | 45.662 | 0.303              | 0.0011                | 323.35 | 30.204 | 0.91               | 0.0024                |
| 283.15 | 68.917 | 0.439              | 0.0018                | 323.15 | 61.349 | 1.84               | 0.0047                |
| 283.25 | 94.385 | 0.583              | 0.0023                | 323.15 | 85.958 | 2.52               | 0.0065                |

**Table 5.** Solubility (mole fraction) and associated uncertainty of N<sub>2</sub> in RP5.

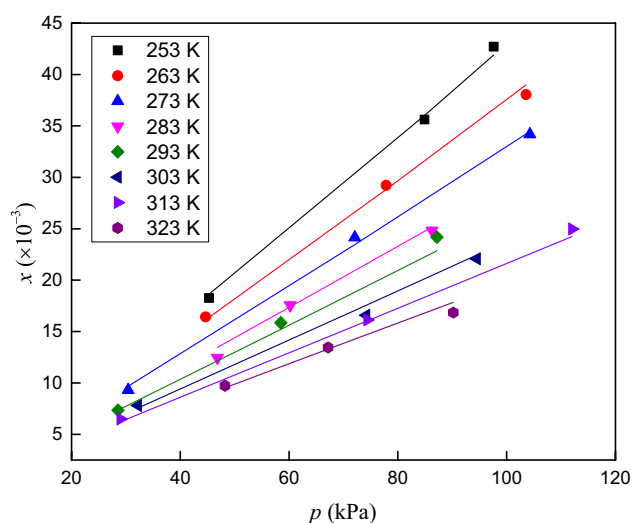


**Figure 4.** Solubility (mole fraction) of CO<sub>2</sub> in RP5 versus temperature and pressure.

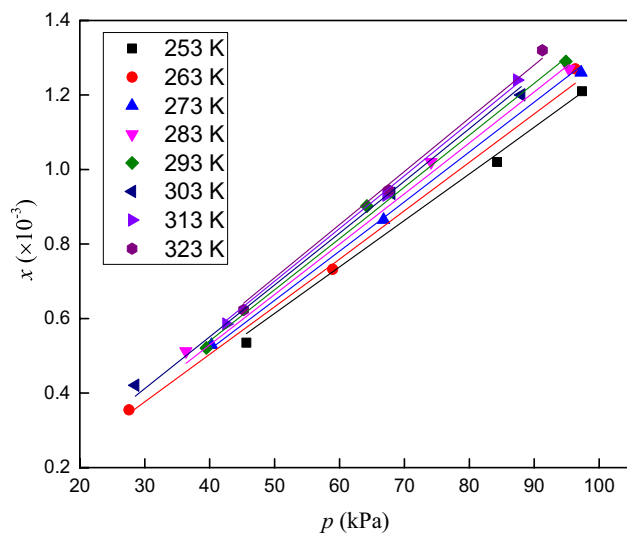


**Figure 5.** Solubility (mole fraction) of O<sub>2</sub> in RP5 versus temperature and pressure.

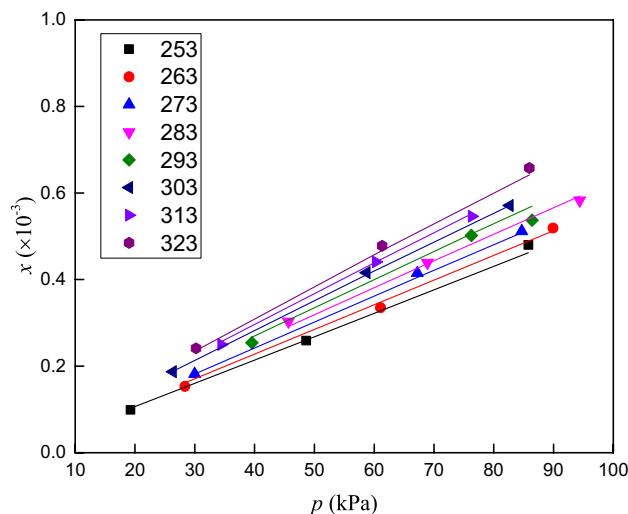


**Figure 6.** Solubility (mole fraction) of N<sub>2</sub> in RP5 versus temperature and pressure.

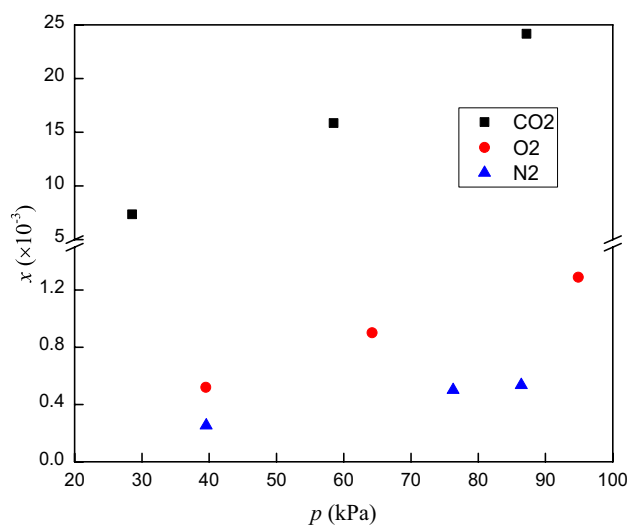


**Figure 7.** Solubility (mole fraction) of CO<sub>2</sub>, O<sub>2</sub> and N<sub>2</sub> in RP5 at 293.15 K.

$$\ln \frac{f(T,p)}{x} = \ln H + \frac{V_1^\infty (p - p_2^s)}{RT} \quad (10)$$

where  $f(T,p)$  is the gas fugacity at the given temperature and pressure, MPa;  $H$  is Henry's constant, MPa;  $V_1^\infty$  is the partial molar volume of the gas in the respective solvent, L/mol;  $p_2^s$  is the saturated vapor pressure of the solvent, MPa; and  $R$  is the gas constant, 8.314 J/(mol K). The gas fugacity can be obtained using REFPROP 9.1 software<sup>21</sup>. The  $p_2^s$  term can be neglected over the very low temperature range used in the experiment.

Henry's constant and  $V_1^\infty$  can both be expressed as functions of the temperature as follows:

$$\ln H = A + \frac{B}{T} \quad (11)$$

$$V_1^\infty = a + bT + cT^2 \quad (12)$$

where  $A$ ,  $B$ ,  $a$ ,  $b$ , and  $c$  are adjustable parameters.

The modified Krichevsky–Kasarnovsky equation can be expressed as follows:

$$\ln \frac{f}{x} = A + \frac{B}{T} + \frac{(a + bT + cT^2)p}{RT} \quad (13)$$

| Parameters                            | CO <sub>2</sub> | O <sub>2</sub> | N <sub>2</sub> |
|---------------------------------------|-----------------|----------------|----------------|
| A/MPa                                 | 4.134           | 3.699          | 3.349          |
| B/MPa                                 | - 812.309       | 180.814        | 478.239        |
| a/J mol <sup>-1</sup>                 | - 12,427.616    | 21,008.713     | - 15,786.025   |
| b/J mol <sup>-1</sup> K <sup>-1</sup> | 54.231          | - 155.212      | 80.847         |
| c/J mol <sup>-1</sup> K <sup>-2</sup> | - 0.050         | 0.277          | - 0.079        |

**Table 6.** Parameters obtained by fitting experimental data.

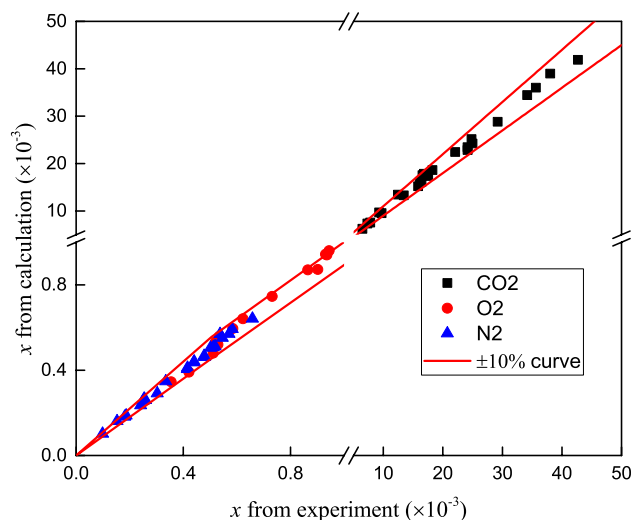


**Figure 8.** Deviation between experimental data (mole fraction) and value calculated using Eq. (13).

Equation (13) can be used to obtain correlations for the individual solubilities of the three gases in RP5. Table 6 presents the adjustable parameters obtained by fitting the experimental data. Figure 8 shows the deviation between the experimental data and the value calculated using Eq. (13).

The deviation between the experimental data and the calculated values is less than 10%. The absolute average deviations (AADs) and maximum deviations (MDs) are determined to analyze the accuracy of the solubility calculated by the modified KK equation. The AAD and MD are expressed below:

$$\text{AAD} = \frac{\sum_i^N \left| \frac{x_{\text{exp}} - x_{\text{cal}}}{x_{\text{exp}}} \right|}{N} \times 100\% \quad (14)$$

$$\text{MD} = \max \left( \frac{x_{\text{exp}} - x_{\text{cal}}}{x_{\text{exp}}} \times 100\% \right) \quad (15)$$

where  $x_{\text{exp}}$  and  $x_{\text{cal}}$  are the experimental and calculated mole fractions of gas in RP5, respectively, and N is the number of experimental data points.

The AADs for CO<sub>2</sub>, O<sub>2</sub> and N<sub>2</sub> are 2.74%, 2.25% and 2.17%, respectively. The MD values for CO<sub>2</sub>, O<sub>2</sub> and N<sub>2</sub> are 8.04%, 7.03% and 6.18%, respectively. Table 7 and Fig. 9 show the values of Henry's constant calculated using Eq. (11) for CO<sub>2</sub>, O<sub>2</sub> and N<sub>2</sub>. Henry's constant decreases as the temperature increases for O<sub>2</sub> and N<sub>2</sub> but increases with the temperature for CO<sub>2</sub>, that similar to the trend of CO<sub>2</sub>, O<sub>2</sub> and N<sub>2</sub> solubility in JP-10 in literature<sup>18</sup>. Henry's constant for the three gases in RP5 decreases in the order N<sub>2</sub> > O<sub>2</sub> > CO<sub>2</sub>, which is opposite to the trend observed for the solubility.

## Conclusions

The isochoric saturation method was used to measure the solubilities of CO<sub>2</sub>, O<sub>2</sub> and N<sub>2</sub> in RP5 at temperatures ranging from 253.15 to 323.15 K and pressures ranging from 0 to 120 kPa. The solubility, as represented by the gas mole fraction, decreases with increasing temperature for CO<sub>2</sub> and increases with the temperature for O<sub>2</sub> and N<sub>2</sub>. The solubilities for the three gases decrease in the order CO<sub>2</sub> > O<sub>2</sub> > N<sub>2</sub> at the same temperature and pressure. The solubilities calculated using the modified KK equation are in good agreement with the experimental data. The absolute average deviations for CO<sub>2</sub>, O<sub>2</sub> and N<sub>2</sub> are 2.74%, 2.25% and 2.17%, respectively. Henry's constant increases with the temperature for CO<sub>2</sub> and decreases with increasing temperature for O<sub>2</sub> and N<sub>2</sub>, which



| T/K    | H/MPa           |                |                |
|--------|-----------------|----------------|----------------|
|        | CO <sub>2</sub> | O <sub>2</sub> | N <sub>2</sub> |
| 253.15 | 2.52            | 82.54          | 188.32         |
| 263.15 | 2.85            | 80.33          | 175.28         |
| 273.15 | 3.19            | 78.33          | 163.99         |
| 283.15 | 3.54            | 76.52          | 154.16         |
| 293.15 | 3.91            | 74.87          | 145.53         |
| 303.15 | 4.28            | 73.37          | 137.91         |
| 313.15 | 4.66            | 71.98          | 131.13         |
| 323.15 | 5.05            | 70.71          | 125.08         |

**Table 7.** Henry's constant for CO<sub>2</sub>, O<sub>2</sub> and N<sub>2</sub> in RP5.

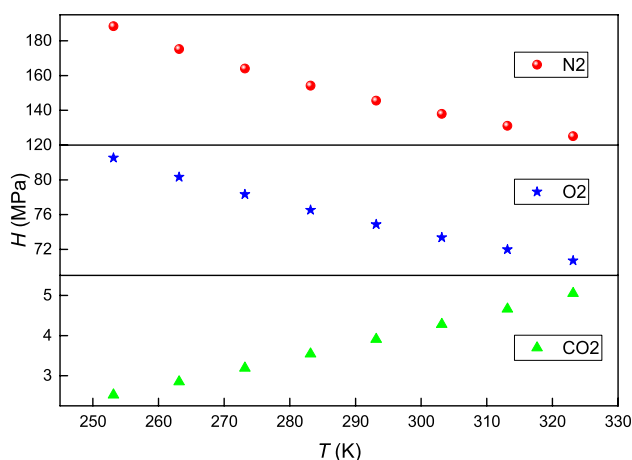


**Figure 9.** Henry's constant versus temperature for CO<sub>2</sub>, O<sub>2</sub> and N<sub>2</sub> in RP5.

represents an opposite trend to that observed for the solubility. Henry's constant for the three gases decreases in the order  $N_2 > O_2 > CO_2$  at the same temperature.

### Data availability

All data generated or analysed during this study are included in this published article.

Received: 21 March 2021; Accepted: 7 March 2022

Published online: 16 March 2022

### References

1. Pei, Y. & Shi, B. Method for analyzing the effect of projectile impact on aircraft fuel tank inerting for survivability design. *Proc. Inst. Mech. Eng. Part G J. Aerosp.* **230**, 2345–2355 (2016).
2. Cavage, W. M. The effect of fuel on an Inert ullage in a commercial transport airplane fuel tank. Federal Aviation Administration, Washington, DC; 2005. Report No.: DOT/FAA/AR-05/25.
3. Kurokawa, F. Y., Andrade, C. R. & Zaparoli, E. L. Modeling of aircraft fire suppression system. *Aircr. Eng. Aerosp. Technol.* **88**, 535–539 (2016).
4. Keim, M., Kallo, J. & Friedrich, K. A. Multifunctional fuel cell system in an aircraft environment: An investigation focusing on fuel tank inerting and water generation. *Aerosp. Sci. Technol.* **29**, 330–338 (2013).
5. Renouard-Vallet, G. N. L., Saballus, M. & Schmithals, G. Improving the environmental impact of civil aircraft by fuel cell technology: concepts and technological progress. *Energy Environ. Sci.* **3**, 1458 (2010).
6. Li, C. Y., Feng, S. Y. & Shao, L. Experimental study of the solubility and diffusivity of CO<sub>2</sub> and O<sub>2</sub> in RP-3 jet fuel. *Aircr. Eng. Aerosp. Technol.* **91**, 216–224 (2019).
7. Feng, S. Y., Peng, X. T. & Chen, C. Effect of air supplementation on the performance of an onboard catalytic inerting system. *Aerosp. Sci. Technol.* **97**, 1–8 (2020).
8. Li, C. Y., Feng, S. Y. & Shao, L. Measurement of the diffusion coefficient of water in RP-3 and RP-5 jet fuels using digital holography interferometry. *Int. J. Thermophys.* **39**, 1–10 (2018).
9. Howlader, M. S., French, W. T. & Toghiani, H. Measurement and correlation of solubility of carbon dioxide in triglycerides. *J. Chem. Thermodyn.* **104**, 252–260 (2017).
10. Diamond, L. W. & Akinfiev, N. N. Solubility of CO<sub>2</sub> in water from –1.5 to 100 °C and from 0.1 to 100 MPa: Evaluation of literature data and thermodynamic modelling. *Fluid Phase Equilibria.* **208**, 265–290 (2003).
11. Barth, J. *et al.* Solubility of natural gas in diesel fuel. *Chem. Eng. Technol.* **39**(8), 1545–1550 (2016).
12. Baird, Z. S. *et al.* Hydrogen solubility of shale oil containing polar phenolic. *Ind. Eng. Chem. Res.* **56**(30), 8738–8747 (2017).

13. Hamme, R. C. & Emerson, S. R. The solubility of neon, nitrogen and argon in distilled water and seawater. *Deep-Sea Res. Part I* **51**, 1517–1528 (2004).
14. Mokhtarani, B. & Gmehling, J. (Vapour+liquid) equilibria of ternary systems with ionic liquids using headspace gas chromatography. *J. Chem. Thermodyn.* **42**, 1036–1038 (2010).
15. Huang, W., Du, X. & Zheng, D. CO<sub>2</sub> Solubility in physicochemical absorbent: dibutyl ether/N-methylethanolamine/ethanol. *Int. J. Thermophys.* **40**, 1–16 (2019).
16. Mahboubeh, P. *et al.* Using static method to measure tolmetin solubility at different pressures and temperatures in supercritical carbon dioxide. *Sci. Rep.* **10**, 19595 (2020).
17. Fandinno, O., Lopez, E. R. & Lugo, L. Solubility of carbon dioxide in two pentaerythritol ester oils between (283 and 333) K. *J. Chem. Eng. Data* **53**, 1854–1861 (2008).
18. Liu, X., Liu, S. & Bai, L. Measurement and correlation of the solubilities of oxygen, nitrogen, and carbon dioxide in JP-10. *J. Chem. Eng. Data* **62**, 3998–4005 (2017).
19. Jia, T., Bi, S. & Wu, J. Solubilities of carbon dioxide, oxygen, and nitrogen in aqueous ethylene glycol solution under low pressures. *Fluid Phase Equilibria* **485**, 16–22 (2019).
20. Shokouhi, M., Jalili, A. H. & Zoghi, A. T. Experimental investigation of hydrogen sulfide solubility in aqueous sulfolane solution. *J. Chem. Thermodyn.* **106**, 232–242 (2017).
21. Lemmon, E. W., Huber, M. L. & McLinden, M. O. *NIST Reference Fluid Thermodynamic and Transport Properties-REFPROP, Version 9.1* (National Institute of Standards and Technology, 2013).
22. Technology NIOS. *Guidelines for Evaluating and Expressing the Uncertainty of NIST Measurement Results* (1994).
23. Carroll, J. J. & Mather, A. E. The system carbon dioxide-water and the Krichevsky–Kasarnovsky equation. *J. Solut. Chem.* **21**, 607–621 (1992).
24. Zhang, J. & Huang, K. Densities and viscosities of, and NH<sub>3</sub> solubilities in deep eutectic solvents composed of ethylamine hydrochloride and acetamide. *J. Chem. Thermodyn.* **139**, 1–8 (2019).

## Acknowledgements

This study was financially supported by NSFC-Civil Aviation Joint Research Fund (U1933121); Natural Science Foundation of Institutions of Higher Education of Jiangsu Province, China (21KJD620003); High-level talent work start-up fee funded project of the Jinling Institute of Technology of China (jit-b-202044); Natural Science Foundation of Institutions of Higher Education of Jiangsu Province, China (18KJD440001); Key Laboratory of Aircraft environment control and life support, Ministry of Industry and Information Technology, Nanjing University of Aeronautics and Astronautics (KLAECLS-E-201903).

## Author contributions

L.C.: writing-draft, measurements; F.S.: Analysis, writing-draft; X.L.: Experimental analysis; P.X.: Analysis, conceptualization; L.W.: Modelling, validation. All authors reviewed the manuscript.

## Competing interests


The authors declare no competing interests.

## Additional information

**Correspondence** and requests for materials should be addressed to S.F.

**Reprints and permissions information** is available at [www.nature.com/reprints](http://www.nature.com/reprints).

**Publisher's note** Springer Nature remains neutral with regard to jurisdictional claims in published maps and institutional affiliations.

 **Open Access** This article is licensed under a Creative Commons Attribution 4.0 International License, which permits use, sharing, adaptation, distribution and reproduction in any medium or format, as long as you give appropriate credit to the original author(s) and the source, provide a link to the Creative Commons licence, and indicate if changes were made. The images or other third party material in this article are included in the article's Creative Commons licence, unless indicated otherwise in a credit line to the material. If material is not included in the article's Creative Commons licence and your intended use is not permitted by statutory regulation or exceeds the permitted use, you will need to obtain permission directly from the copyright holder. To view a copy of this licence, visit <http://creativecommons.org/licenses/by/4.0/>.

© The Author(s) 2022